Photochemistry and Photobiology, 20**, **: *–*

Solvent and media effects on the photophysics of naphthoxazole derivatives†

Manuel Curitol[1], Xavier Ragas[2], Santi Nonell[2], Nancy Pizarro[3], María V. Encinas[4], Pedro Rojas[1], Renzo P. Zanocco[1], Else Lemp[1], Germán Günther[1] and Antonio L. Zanocco*[1]

[1]Facultad de Ciencias Químicas y Farmacéuticas, Departamento de Química Orgánica y Fisicoquímica, Universidad de Chile, Santiago, Chile
[2]Grup d'Enginyeria Molecular, Institut Químic de Sarrià, Universitat Ramon Llull, Barcelona, España
[3]Facultad de Ecología y Recursos Naturales, Departamento de Ciencias Químicas, Universidad Andrés Bello, Santiago, Chile
[4]Facultad de Química y Biología, Universidad de Santiago de Chile, Santiago, Chile

Received 28 March 2013, accepted 2 July 2013, DOI: 10.1111/php.12133

ABSTRACT

The photophysical properties of 2-phenyl-naphtho[1,2-d][1,3] oxazole, 2(4-N,N-dimethylaminophenyl)naphtho[1,2-d][1,3] oxazole and 2(4-N,N-diphenylaminophenyl) naphtho[1,2-d] [1,3]oxazole were studied in a series of solvents. UV–Vis absorption spectra are insensitive to solvent polarity whereas the fluorescence spectra in the same solvent set show an important solvatochromic effect leading to large Stokes shifts. Linear solvation energy relationships were employed to correlate the position of fluorescence spectra maxima with microscopic empirical solvent parameters. This study indicates that important intramolecular charge transfer takes place during the excitation process. In addition, an analysis of the solvatochromic behavior of the UV–Vis absorption and fluorescence spectra in terms of the Lippert–Mataga equation shows a large increase in the excited-state dipole moment, which is also compatible with the formation of an intramolecular charge-transfer excited state. We propose both naphthoxazole derivatives as suitable fluorescent probes to determine physicochemical microproperties in several systems and as dyes in dye lasers; consequence of their high fluorescence quantum yields in most solvents, their large molar absorption coefficients, with fluorescence lifetimes in the range 1–3 ns as well as their high photostability.

INTRODUCTION

There are many studies focused on the photophysical properties of benzoxazole derivatives, from a basic perspective to the development of molecules with suitable properties to be employed in diverse applications (1–4). Early studies explore the absorptive and emissive characteristics of 2-phenylbenzoxazole and its p-substituted derivatives with the aim of accounting for their capacities as near-UV laser generators. This application is strongly supported by the high fluorescence quantum yields, the efficient laser output and the extreme photostability of this class of dyes (5–10). Absorption and emission spectra of 2-phenylbenzoxazole and its derivatives (substituted with electron donor groups in the para position on the phenyl ring) possess well-resolved vibrational structure in nonpolar solvents. This is the result of a bond order higher than one between C-2 in the heterocyclic ring and the phenyl substituent, which restricts rotation of two aromatic subunits of 2-phenylbenzoxazole (11). The presence of an electron donor substituent in a phenyl ring of 2-phenylbenzoxazole shifts both the absorption and emission spectra to longer wavelengths. The major shift of the fluorescence spectrum can be explained in terms of charge transfer in the excited state from the phenyl ring to the benzoxazole moiety (11). The highly favorable photophysical properties of this type of heterocyclic compounds, high fluorescence quantum yield, photostability, as well as their easy tuning of photophysical properties (by changing a substituent at position two of benzoxazole ring) made this compounds very useful in the search of new fluorophores. Consequently, benzoxazole derivatives have been used as organic plastic scintillators (12) and optical fiber sensors (13,14). Moreover, some of the derivatives are biologically active, showing activity as cytotoxic (15,16), antimicrobial (17,18), inhibitors of both eukaryotic DNA topoisomerase I and II (19) and genotoxic (20). They have also been used as fluorescent probes for thiols (21–24) and metal cations (25,26) quantitation in biological samples. The long-wavelength absorption and emission bands and high fluorescence quantum yield of benzoxazol-5-yl-alanine derivatives allow their use as fluorescent markers in biological systems, even in the presence of tryptophan (27,28). Benzoxazole derivatives also are an efficient tool for monitoring and exploring the properties of micelles and the hydrophobic interactions in human serum albumin (29), and to produce polymeric nonlinear optical materials with large hyperpolarizability values (30,31). Furthermore, polybenzoxazole derivatives have been proposed as positive photosensitive precursors for applications in microelectronics (32), in electroluminescent devices (2,33), and for the generation of linearly polarized light using the autoorganization capability of liquid crystalline media (34). In spite of the wide range of basic and innovative research that has been developed having as center the emissive properties of benzoxazole, no reports describe the photophysics and/or the photochemistry of compounds with the oxazole heterocycle condensed to extended aromatic systems. There are a variety of synthetic methods to obtain naphthoxazole derivatives (35–40),

*Corresponding author email: azanocco@ciq.uchile.cl (Antonio L. Zanocco)
†This article is part of the Special Issue dedicated to the memory of Elsa Abuin.

however, the only study related to naphthoxazole photophysics involves the use of 1,2-naphthozaxoles as substitutes for the benzoxazole residue in merocyanine 540. This change increases the fluorescence and triplet yields and decreases concomitantly the yield for photoisomerization (41). Also, naphthoxazole derivatives have been used to fine-tune the phosphorescence color in a series of heteroleptic Ir(III) complexes (42). Building on the fact that the benzoxazole excited states have substantial charge-transfer character, we hypothesized that substitution of the benzo- with a naphtho group could markedly affect the photophysical properties of the aryloxazoles. In addition, inclusion of an electron donor substituent also should enhance the intramolecular charge transfer in the excited singlet state. With this aim, we synthesized three naphthoxazole derivatives (Fig. 1) and studied the solvent effect on their absorption and emission. The properties evaluated for these compounds suggest that they are valuable candidates for technological applications such as laser dyes, quantum counters or fluorescent probes.

MATERIALS AND METHODS

General. All solvents used in syntheses, spectroscopic and kinetic measurements were of reagent grade, spectroscopic or high performance liquid chromatography quality. Nuclear magnetic resonance (NMR) spectra were recorded in a Bruker Advance 300 MHz spectrometer. Chemical shifts are referred to the internal standard tetramethylsilane (TMS). A Hewlett Packard 5890 gas chromatograph equipped with a nitrogen-phosphorus detector and a capillary column was employed in gas-liquid chromatography experiments. Steady-state fluorescence spectra were recorded in a Fluorolog 2 Tau 2 spectrofluorometer. Fluorescence lifetime measurements were carried out with the time correlated single-photon counting technique using an Edinburgh Instruments OB-900 or a Pico-Quant Fluotime 200 fluorescence lifetime spectrometers.

Chemical synthesis. Naphthoxazole derivatives were synthesized employing a modification in a method previously described in the literature (40).

2-phenyl-naphtho[1,2-d][1,3]oxazole (NX1). A solution of 2-nitroso-naphthol, 180 mg (1.03 mmol), in absolute ethanol (EtOH) (ca. 30 mL) was stirred with 10% (w/w) Pd/C catalyzer under hydrogen at room temperature. The mixture was protected from light, and the reaction progress was followed by TLC. After complete consumption of the starting material (ca. 2 h), the excess of hydrogen was removed by flushing with a nitrogen current. Then, 0.15 mL (1.48 mmol) of benzaldehyde in absolute EtOH was added and the mixture was refluxed for 20 h under nitrogen. After cooling down to room temperature, 1.5 mmol of 2,3-dichloro-5,6-dicyano-1,4-benzoquinone (DDQ) was added carefully and additionally stirred for 5 min at room temperature. Then, the solid residue was filtered out and the ethanolic solution extracted with methylene chloride. The extract was dried over magnesium sulfate and the solvent was evaporated under reduced pressure. Purification by column chromatography yields 53% of 2-phenyl-naphtho[1,2-d][1,3]oxazole, m.p. 123–124°C. Lit. (39) 122–123°C. ^{1}H-NMR ($CDCl_3$) δ: 8.60 (d, J_d 8.20 Hz, 1H), 8.34 (m, 2H), 7.99 (d, J_d 8.20 Hz, 1H), 7.82 (d, J_d 8.90 Hz,1H), 7.76 (d, J_d 8.90 Hz, 1H), 7.69 (m, 1H), 7.56 (m, 4H). ^{13}C-NMR (CDCl3) δ: 162.7, 148.5, 131.7, 131.5, 129.3, 128.9, 127.9, 127.8, 127.4, 127.0, 126.4, 125.8, 122.7, 111.2.

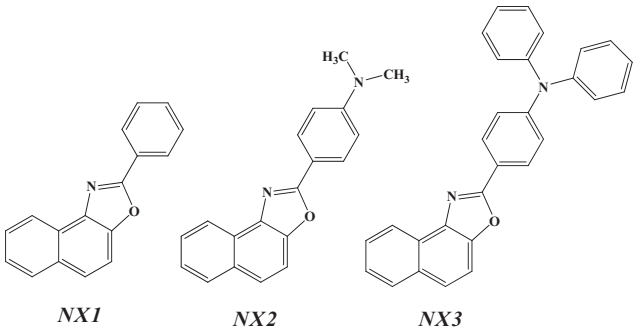

Figure 1. Chemical structures of the studied naphthoxazole derivatives.

2(4-N,N-dimethylaminophenyl)naphtho[1,2-d][1,3]oxazole (NX2). Using the same procedure described above, 2-nitrosonaphthol, 180 mg (1.03 mmol) and p-dimethylaminobenzaldehyde, 223 mg (1.5 mmol) yield 38% of 2(4-N,N-dimethylaminophenyl) naphtho[1,2-d][1,3]oxazole, m.p. 182–183°C. Lit. (41) 177–179°C ^{1}H-NMR ($CDCl_3$) δ: 8.57 (d, J_d 8.2 Hz, 1H), 8.20 (d, J_d 8.8 Hz, 2H), 7.95 (d, J_d 8.2 Hz, 1H), 7.72 (d, J_d 8.8 Hz, 2H), 7.64 (m, 1H), 7.50 (t, J_t 7.5 Hz, 1H), 6.81 (d, J_d 8.8 Hz, 2H), 3.07 (s, 6H). ^{13}C-NMR ($CDCl_3$) δ: 167.7, 155.2, 150.7, 141.0, 134.2, 131.9, 129.7, 129.4, 128.1, 127.7, 125.4, 120.1, 117.9, 114.8, 113.8, 43.2.

2(4-N,N-diphenylaminophenyl)naphtho[1,2-d][1,3]oxazole (NX3). Employing a similar method as described above, 2-nitrosonaphthol, 180 mg (1.03 mmol) and p-diphenylaminobenzaldehyde, 410 mg (1.5) mmol, yield 52% of 2(4-N,N-diphenylaminophenyl) naphtho[1,2-d][1,3]oxazole, m.p. 204–206°C. ^{1}H-NMR (CDCl3) δ: 8.42 (d, J_d 8.5 Hz, 1H), 8.12 (m, 3H), 7.95 (s, 2H), 7.71 (t, J_t 7.2 Hz, 1H), 7.60 (t, J_t 7.2 Hz, 1H), 7.42 (t, J_t 8.9 Hz, 6H), 7.20 (d, J_d 8.2 Hz, 2H), 7.06 (d, J_d 8.6 Hz 4H).

Instrumental methods. Fluorescence quantum yields (Φ_F) were measured by the comparative method described by Eaton and Demas *et al.* (43,44), using quinine sulfate in 0.1 N sulfuric acid (Φ_F = 0.55) as reference. Optical densities of sample and reference solutions were set below 0.2 at the excitation wavelength and the fluorescence spectra were corrected using rhodamine G as reference. Sample quantum yields were evaluated by using Eq. (1):

$$\Phi_x = \left(\frac{\mathrm{Grad_x}}{\mathrm{Grad_{Act}}}\right)\left(\frac{\eta_x^2}{\eta_{Act}^2}\right)\Phi_{Act} \qquad (1)$$

where $\mathrm{Grad_x}$ and $\mathrm{Grad_{Act}}$ are the slope of integrated fluorescence vs. absorbance plots for the sample and the actinometer, and η_x and η_{Act} are the refractive index of sample and actinometer solutions respectively. All measurements were carried out in nitrogen-purged solutions at (20.0 ± 0.5)°C. Geometry optimizations, energy evaluation and Franck–Condon transition calculations were carried out with Gaussian 09W (45).

RESULTS AND DISCUSSION

Absorption spectra

The absorption spectra of the naphthoxazole derivatives 2-phenyl-naphtho[1,2-d][1,3]oxazole (NX1), 2(4-N,N-dimethylaminophenyl) naphtho[1,2-d][1,3]oxazole (NX2) and 2(4-N,N-diphenylaminophenyl)naphtho[1,2-d][1,3]oxazole (NX3) were determined in a

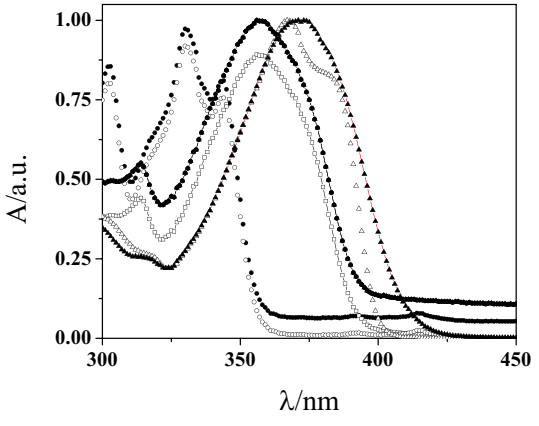

Figure 2. Absorption spectra of 2-phenyl-naphtho[1,2-d][1,3]oxazole (NX1) (●),2(4-N,N-dimethylaminophenyl)naphtho[1,2-d][1,3]oxazole (NX2) (■) and 2(4-N,N-diphenylaminophenyl)naphtho[1,2-d][1,3]oxazole (NX3) (▲) in benzene and methanol as solvents. Open symbols correspond to the spectra in methanol.

large set of solvents of different polarity and proton donating capacity at room temperature. Figure 2 shows the absorption spectra in benzene and methanol as examples of nonpolar and polar protic solvents respectively. The determined corresponding spectral data are summarized in Table S1.

NX1, NX2 and NX3 display absorption spectra with an intense and broad low-energy band in the range 310–360, 320–390 and 325–415 nm respectively. The molar extinction coefficients at the maximum wavelength are high, ranging between (7.98–30.40) $\times$ 10^3 M^{-1} cm^{-1}, (11.79–52.95) $\times$ 10^3 M^{-1} cm^{-1} and (35.22–61,09) $\times$ 10^3 M^{-1} cm^{-1} for NX1, NX2 and NX3 respectively. The maximum absorption wavelength is almost insensitive to the solvent polarity, being more relevant to the profuse vibrational fine structure observed in NX1 spectrum; this behavior is probably due to the limited rotation of the bond between the oxazole ring and the 2-phenyl substituent (bond order greater than one) (7,11). We performed spectra calculations employing the density functional theory (DFT) formalism (B3LYP-6311g+ for structure optimization) and ZINDO-S, CIS and TD-SCF to calculate the vertical Franck–Condon transitions.

Calculations performed with ZINDO-S method overestimate λ_{max} by about of 10–30 nm, whereas CIS (631 g basis) underestimate λ_{max} values by a larger amount. Better results were obtained using TD-SCF (DFT 6311+g) level of theory, from which vertical transitions at 339.8 nm (f = 0.61), 357.0 nm (f = 0.85) and 379.7 (f = 9.1) are predicted for NX1, NX2 and NX3, in good agreement with the experimental values. In addition, molecular orbital analysis indicates a π–π* transition for these molecules. These results are consistent with those previously reported for benzoxazole derivatives (46) and structurally related compounds such as benzoxazinones (47) and coumarins (48).

Emission spectra

NX1, NX2 and NX3 exhibit intense emission spectra. The position of the fluorescence maximum is strongly affected by the solvent, a red shift being observed upon increasing the solvent polarity (Fig. 3). Such behavior indicates that the fluorescent state would be a highly polar state with an important charge-transfer character. The relevant emission parameters in the solvent set employed are included in Table S2.

A deeper rationalization of solvent-induced shift of the fluorescence spectra can be obtained from the analysis of the fluorescence maximum dependence on microscopic solvent parameters

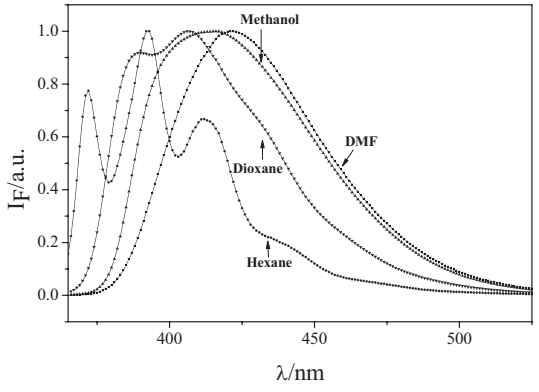

Figure 3. Normalized fluorescence spectra of NX2 in solvents representatives of the polarity scale.

by employing linear solvation relationship (LSER) and/or theoretical linear solvation relationship (TLSER) equations. We employed the semiempirical solvatochromic equation (LSER) of Kamlet *et al.* Eq. (2) (49–51):

$$\bar{\nu}_F = \bar{\nu}_0 + a\pi^* + d\delta + b\alpha + c\beta + h\rho_H^2 \qquad (2)$$

In Eq. (2), π* accounts for polarizabilities and dipolarities of solvent (52,53), δ is a correction term for polarizability, α corresponds to the hydrogen bond donor solvent ability, β indicates solvent capability as a hydrogen bond acceptor and ρ_H is the Hildebrand parameter, a measure of disruption of solvent–solvent interactions in creating a cavity (50). The coefficients of the LSER equation (Eq. (2)) obtained by multilinear regression analysis of the dependence of $\bar{\nu}_F$ on the solvent parameters are given in Table S3. This analysis is supported by purely statistical criteria. To sum up, sample size, N, product correlation coefficient, R, standard deviation, SD and the Fisher index of equation reliability, F indicate the quality of the overall correlation equation. The reliability of each term is indicated by t-statistic, t-stat and the variance inflation factor (VIF). Suitable quality is indicated by large N, F and t-stat values, small SD values and R and VIF values close to one (54). Also, we analyzed the dependence of the fluorescence maximum on solvent using a theoretical set of correlation parameters determined solely from computational methods (55–57). The TLSER descriptors have been developed to give optimal correlation with LSER descriptors. The generalized TLSER equation proposed by Famini *et al.* (55–57), (Eq. 3) can be used to analyze dependence emission maxima on solvent properties.

$$\bar{\nu}_F = \bar{\nu}_0 + a\pi_1 + b\varepsilon_b + cq_- + d\varepsilon_a + eq_+ + h\rho_H^2 \qquad (3)$$

In Eq. (3), the bulk/steric term is described by the Hildebrand parameter, ρ_H. The parameter π_1 corresponds to the index of polarizability and accounts for the ease of moving (or polarizing) of the electron cloud, and is obtained from the ratio between polarizability volume and molecular volume. The hydrogen bond acceptor basicity (HBA) involves covalent, ε_b, and electrostatic, q_-, terms. Similarly, hydrogen bond donor acidity (HBD) includes covalent, ε_a, and electrostatic, q_+, terms (57). The coefficients of the LSER and TLSER equations obtained by multilinear regression analysis for the dependence of the fluorescence maximum on solvent parameters are given in Table S3.

Results (Table S3) show that not all descriptors are statistically relevant. Descriptor coefficients accepted in the correlation equation were those having significance level $\geq$0.95. Accordingly, the ρ_H and β parameters were discarded in LSER correlation for NX1 and NX3. Furthermore, ρ_H was not included in LSER correlation for NX2. According to the LSER coefficients in Table S3, the energy of the fluorescent state decreases in solvents with largest capacity to stabilize charges and dipoles and in strong HBD solvents. In addition, for NX2 the energy of the fluorescent state also decreases in HBA solvents. This results support an emissive state with a strong intramolecular charge-transfer character which is stabilized in π* solvents. Further stabilization of the excited state is obtained from the interactions of HBD solvents with the most negative center of the molecule, probably the oxygen atom in the oxazole ring. Dependence of the emission wavelength on the β parameter for NX2 can be explained in terms of HBA solvent interactions with the most

positive center of the excited molecule, probably the dimethylamino substituent. Similarly, only q_-, ε_a and q_+ were statistically relevant in the TLSER study. The TLSER treatment (Table S3) shows that HBD and HBA solvents increase the emission wavelength for all NX1, NX2 and NX3. In the TLSER treatment $\pi 1$ (not included in our correlation equations of Table S3) models the solvent ability to stabilize dipole-induced dipole and induced dipole-induced dipole interactions. No adequate TLSER model for dipolarity itself has been found. The TLSER analysis indicates that the influence of HBA solvents is mainly electrostatic because only q_- is included in the correlation equation, whereas HBD solvents shift the fluorescence maximum by means of electrostatic and covalent interactions. The dependence of the wavelength of the fluorescence maximum on ε_a would be explained if considerable negative charge is developed on the oxygen atom in the heterocyclic ring, which HBD solvents can stabilize through predominant hydrogen-bonding interactions. Furthermore, if the positive charge in the excited state is delocalized on the whole aromatic system, no formal bonding interactions with HBA solvents can be expected.

Fluorescence quantum yields for NX1 and NX2 are close to 1 in most solvents (Table S2). Furthermore, fluorescence lifetimes are near to 2 and 1.3 ns for NX1 and NX2, respectively, and are essentially solvent independent because the predominant radiative process is mainly dominated by the aromatic nature of the molecule. For NX3, fluorescence quantum yield shows solvent dependence, diminishing from 1 in nonpolar solvents to around of 0.65 in polar solvents. Concomitantly, the fluorescence lifetimes increase from 1.3–1.5 ns in nonpolar solvents such as hexane or benzene to 3.7–4.2 ns in polar solvents such as methanol or propylencarbonate. These results can be explained if we consider that $\phi_F = k_F/(k_F + k_{nr})$ and $\tau_F = 1/(k_F + k_{nr})$ and the formation of a twisted intramolecular charge transfer (TICT) that opens a nonradiative deactivation pathway due to the rotation of the disubstituted amino group (58). It is well known that the energy barrier for the formation of a TICT state from the locally excited state decreases as the polarity of the medium increases (59,60). As the dipole moment of the TICT state is very large, the dipolar interactions of the TICT state will raise with the increase in the solvent polarity. Thus, the diminution of the fluorescence intensity of NX3 in polar solvents could be due to the large stabilization of the highly polar TICT state by strong dipole–dipole and/or hydrogen-bonding interactions and consequent rapid nonradiative transition to the ground state. This fact diminishes k_F and increases k_{nr}, but the radiative deactivation path remains as the prevailing process in the photophysics of di-N,N-substituted aminophenylnaphthoxazoles. The effect is evident for NX3, but not clearly observed for NX2 because the TICT formation depends on two main factors, the planarity of the molecule and the donor–acceptor character of the substituent, both advantageous for the molecule with the diphenylamino substituent. Independent of these results, the large fluorescence quantum yields and short fluorescence lifetimes found for the naphthoxazole derivatives in a representative set of solvents, make these compounds very promising fluorescent probes to be used in a wide range of microenvironments.

Excited-state dipole moment determination

The spectral shift of the fluorescence, or more rigorously, the difference between the positions of the absorption and fluorescence maxima depends on solvent polarity function defined by dielectric constant (ε) and refractive index (η) of the solvent. The dipole moment change between excited- and ground states can be experimentally calculated from the Lippert–Mataga relationship, if polarizability of the solute can be neglected, i.e. $\alpha = 0$ (61,62):

$$\bar{\nu}_A - \bar{\nu}_F = m_1 f(\varepsilon, \eta^2) + \text{const.} = m_1 \left(\frac{\varepsilon - 1}{2\varepsilon + 1} - \frac{\eta^2 - 1}{2\eta^2 + 1} \right) + \text{const.} \tag{4}$$

$$m_1 = \frac{(\mu_e - \mu_g)^2}{\kappa a^3} \tag{5}$$

where μ_e and μ_g are the dipole moments of the fluorophore in the excited- and the ground state respectively; a is a radius of the Onsager cavity, assumed to be a sphere and κ is a universal constant equal to 1.10511×10^{-35} C^2. For those spectra in which the maximum is not well defined due to the fine structure or shoulders appearance, the maximum wavelength of the lower energy band was obtained using a convolution method. A representative Lippert–Mataga plot for NX1 is shown in Fig. 4. At this point, it must be stated that, according to the results of the solvent effect, the stabilization of fluorescent excited state not only depends on electric factors. Solvent acidity and basicity also lower the energy (affecting the maximum wavelength). So, determinations by using Lippert–Mataga relationship in this case, probably overestimate the magnitude of excited dipole moments.

Based on the calculated values of Onsager's cavity radius and the ground-state dipole moment for NX1, NX2 and NX3 using DFT B3LYP (6311+g) to minimize the molecular geometry, the excited-state dipole moments were calculated from the slopes of Lippert–Mataga plots. Results obtained from these experiments, summarized in Table 1, show a significant increase in the dipole moment in the singlet excited state. Thus, a relatively large charge transfer takes place during the excitation of the oxazole derivatives. The larger dipole moments obtained for both NX2 and NX3 for the ground and the excited state reflect the donor effect of the dimethyl and diphenylamino group on the phenyl substituent, implying that both naphthalene moiety and phenyl substituent in position 2 are involved in the charge-transfer

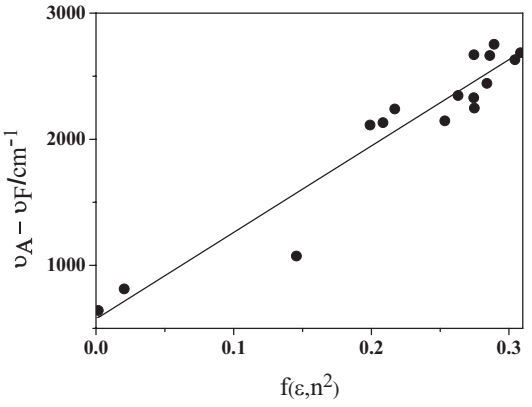

Figure 4. Lippert–Mataga plot of the difference between the maximum of the absorption and fluorescence on the solvent polarity function, $f(n^2, \varepsilon) = (((\varepsilon - 1)/(2\varepsilon + 1)) - ((n^2 - 1)/(2n^2 + 1)))$ for 2-phenyl-naphtho[1,2-d][1,3]oxazole.

Table 1. Ground (μ_g) and excited dipolar moments (μ_e) for NX1, NX2 and NX3.

Compound	μ_g/D	a_0 (Å)	$\Delta\mu$/D	μ_e/D
NX1	0.96	5.14	9.61 ± 1.3	10.57 ± 2.0
NX2	3.31	5.67	12.01 ± 1.8	15.32 ± 2.31
NX3	2.01	6.30	14.55 ± 2.1	16.56 ± 2.41

μ_g obtained from DFT B3LYP 6311g+dp minimized structure in gas phase, a_0 calculated from DFT B3LYP 6311g+dp minimized structure, $\Delta\mu$ obtained from the slope of the Lippert–Mataga plot.

process toward the oxazole acceptor center. Similar results for the change in the dipole moment as consequence of an intramolecular charge transfer have been reported for analogous 2-phenyl-benzoxazole derivatives (63,64).

Photostability

Considering the potential use as fluorescent dyes in dye lasers or for single-molecule-based microscopy techniques of the studied compounds, we also evaluated their photostability under extreme irradiation conditions. Photoconsumption quantum yields were evaluated in benzene as solvent, using Aberchrome 540 as actinometer and Exalite 376 (rhodamine 110) as reference. Samples were irradiated with the third harmonic pulses (355 nm) of a Continuum-Surelite II Nd:Yag laser (6 μs, 15 mJ/pulse, 6000 pulses). The concentration changes were monitored by employing gas chromatography and/or UV–Vis spectrophometry. Photoconsumption quantum yields, (the mean of six measurements) for NX1, NX2 and NX3, equal to $(4.6 \pm 0.9) \times 10^{-5}$, $(2.4 \pm 0.6) \times 10^{-5}$ and $(2.1 \pm 0.5) \times 10^{-5}$, respectively, are close to the measured for the extensively used dye rhodamine 110, equal to $(6.7 \pm 1.4) \times 10^{-6}$. These results show that the studied naphthoxazole derivatives are very photostable being appropriate molecules to be used as fluorescent dyes in experiments involving long-term irradiation.

Studies in micellar systems

Self-association of long-chain amphiphilic molecules forms micellar aggregates in aqueous solutions, above certain concentration called critical micelle concentration (CMC). In this section, NX2 and NX3 have been employed to determine the CMC values for the commonly used surfactants sodium dodecyl sulfate (SDS) triton X-100, TX-100 and sucrose monopalmitate (SuMP). The CMC values were calculated from the variation in the relative fluorescence intensities (I_F/I_F^0) with the surfactant concentration, however, the observed change in the fluorescence spectrum with the surfactant addition depends on the surfactant chemical nature. Addition of SDS to an aqueous solution of NX2 and NX3 increases the fluorescence intensity and shifts the emission maxima to the red (Fig. 5), whereas unexpectedly, when TX-100 and SuMP are added, the fluorescence maximum is blue shifted.

This behavior can be rationalized in terms of the NX2 and NX3 localization in the micelle. It is obvious that the probe is not incorporated into the micelle core, otherwise a noteworthy blue shift of the emission maxima (up to approximately 410–420 nm) would be observed due to the nonpolar nature of this microenvironment. From the dependence of the fluorescence maximum with the dielectric constant and the $E_T(30)$ parameter of the solvent, we can estimate the dielectric constant and the

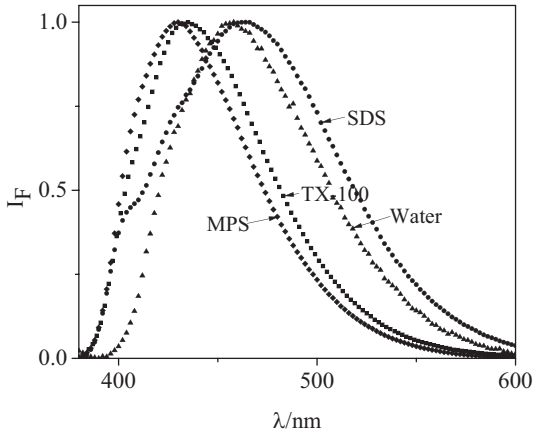

Figure 5. Comparison of the normalized fluorescence spectra of 2(4-N, N-diphenylaminophenyl)naphtho[1,2-d][1,3]oxazole in water and in micellar solution of various surfactants.

$E_T(30)$ values corresponding to the microenvironment in which NX3 locates in SDS, TX-100 and SuMP micellar solutions. With this approximation, we can conclude that NX3 in SDS micellar solutions senses a media similar to dimethylformamide or acetonitrile whereas in TX-100 and SuMP micellar solutions the microenvironment resembles dioxane or tetrahydrofuran, consequently, both probes, NX2 and NX3, should be located near to the micellar interface. Due to the intramolecular charge-transfer nature of the excited NX2 and NX3 state, the disubstituted amino group, $-NR_2$ should have a more positive charge whereas the electron withdrawing naphthoxazole moiety will have a more negative charge. Hence, in SDS micelles, it could be suggested that the $-NR_2$ group is located in the Stern layer (containing the negatively charged sulfate groups) and the naphthoxazole moiety in the Gouy–Chapman layer (including the more positively charged sodium counter ions) (see Figure S1). Similarly, in SuMP micelles the positively charged amino substituent interacts with the carboxyl oxygen of the acid moiety of the surfactant, whereas the oxazole ring localizes between the sucrose head groups where the interactions between the hydroxyl groups and the oxazole ring heteroatoms are very favorable. On the contrary, for the fluorescent probe, 2-(p-dimethylaminostyryl)benzoxazole has been proposed that in TX-100 micelles the $-NR_2$ group is present in the Gouy–Chapman layer, whereas the benzoxazole ring locates in the Stern layer (29). Consequently, red shifting in SDS micelles can be understood in terms of two factors, the stabilization of the probe ground state in water, a process markedly dominated by hydrogen bond interactions, and the greater stabilization of its excited singlet state in the SDS micellar interface where the larger molecular dipole of the excited species makes possible strong interactions with the charged interface. The blue shift observed in TX-100 and SuMP micelles can be explained in a similar fashion. The transference of the probe from the water media to the non-ionic, although rich in hydroxyl groups interface, destabilizes the probe ground state because hydrogen bond interactions are broken. However, an even more important destabilization of the excited probe in the interface should take place, due to the increase in the probe dipole moment with the excitation and the less-polar microenvironment around it as result of the presence of structured water molecules near to surfactant heads. A similar, less-polar, rich in structured

water microenvironment around the TX-100 head groups can be also expected. This picture of the probe location in micellar solutions is further supported by the larger increase in the fluorescence quantum yield in SuMP and TX-100 micelles (Fig. 6). The increase of ϕ_F in SuMP and TX-100 micelles implies that the probe is located in a constrained microenvironment where its mobility is relatively reduced due to the presence of structured water molecules, although probe incorporation in some extension between the hydrophobic tails of surfactant molecules has been also suggested by Fayed (29), studying the absorption and emission characteristics of 2-(p-dimethylaminostyryl) benzoxazole in micellar solutions.

Despite of the emission shift, the CMC values obtained for SDS, TX-100 and SuMP are in good agreement with those obtained using other well-known probes (3,65–67). Figure 6A–C shows the plots obtained for the dependence of the values of I_F/I_F^0 on the SDS, TX-100 and SuMP concentration, monitored at 460, 430 and 441 nm, respectively, when the probe employed was NX3.

From these plots the CMC values included in Table 2 were obtained. When SDS or TX-100 was the surfactant, fluorescence intensity values increase abruptly at the CMC, if the fluorescence changes are followed at the wavelength corresponding to the maximum observed above the CMC and the fluorescence intensity increase was independent of the probe employed. With SuMP the behavior is more complicated as deduced from the plot of I_F/I_F^0. The fluorescence intensity increases gradually from very low SuMP concentration. This behavior can be explained in terms of the probe interactions with the hydroxyl groups of the sucrose head of the surfactant and probably with SuMP aggregates at the premicellization range (68).

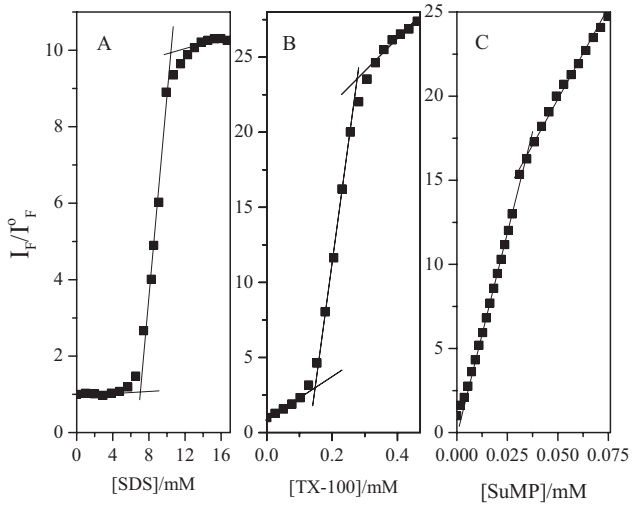

Figure 6. (A) Dependence of the relative fluorescence intensity of 2(4-N,N-diphenylaminophenyl)naphtho[1,2-d][1,3]oxazole (NX3) measured at 460 nm on the SDS concentration, (B) dependence of the relative fluorescence intensity of NX3 measured at 430 nm on the TX-100 concentration, (C) dependence of the relative fluorescence intensity of NX3 measured at 441 nm on the SuMP concentration.

Table 2. CMC values of SDS, TX-100 and SuMP measured using fluorescence techniques.

	CMC (mM)		
Probe	SDS	TX-100	SuMP
NX2	7.9	0.25	0.033
NX3	8.6	0.23	0.034

CONCLUSIONS

The studied naphthoxazole derivatives show valuable spectroscopic and photochemical properties: large molar absorbability and fluorescence quantum yield, short fluorescence lifetime and comparable photostability to commercially available laser dyes. These compounds have a photophysic behavior similar to analogous benzoxazoles, but with larger molar absorptivity's, a small red shift of both the absorption and emission maxima and a larger Stokes shift in polar solvents. These properties in addition to the large solvent–dependent changes in the dipole moment on excitation make these molecules valuable candidates as fluorescent probes to be used in fluorescence microscopy and to determine micellar properties such as CMC or partition constants of added additives (68).

Acknowledgement—Financial support from FONDECYT (grants 1080410 and 1040573) is gratefully acknowledged.

SUPPORTING INFORMATION

Additional Supporting Information may be found in the online version of this article:

Table S1. Detailed absorption characterization of NX1, NX2 and NX3 in solution.

Table S2. Detailed emission characterization of NX1, NX2 and NX3 in solution.

Table S3. Analysis of solvent effect on the emission of NX1, NX2 and NX3 using LSER equations.

Figure S1. Schematic representation of NX3 location in SDS and SuMP micelles.

REFERENCES

1. Astrand, P. O., P. Sommer-Larsen, S. Hvilsted, P. S. Ramanujam, K. L. Bak and S. P. A. Sauer (2000) Five-membered rings as diazo components in optical data storage devices: An *ab initio* investigation of the lowest singlet excitation energies. *Chem. Phys. Lett.* **325**, 115–19.
2. Fehervari, A. F., L. C. Kagumba, S. Hadjikyriacou, F. Chen and R. A. Gaudiana (2003) Photoluminescence and excimer emission of functional groups in light-emitting polymers. *J. Appl. Polym. Sci.* **87**, 1634–45.
3. Quaranta, A., S. M. Carturan, T. Marchi, V. L. Kravchuk, F. Gramegna, G. Maggioni and M. Degerlier (2010) Optical and scintillation properties of polydimethyl-diphenylsiloxane based organic scintillators. *IEEE Trans. Nucl. Sci.* **57**, 891–900.
4. Vincze, A., L. Halasz, J. Solymosi, B. Agai, I. Kasa, A. Molnar and A. Safrany (2007) Development of an extractive-scintillating chromatographic resin for the detection of radioactive isotopes. *J. Radioanal. Nucl. Chem.* **273**, 615–19.
5. Del Valle, J. C., M. Kasha and J. Catalan (1996) Chemical physics of excitation dynamics via amplified spontaneous emission (ASE) laser spike spectroscopy in substituted phenyloxazoles. *Chem. Phys. Lett.* **263**, 154–60.
6. Reiser, A., L. J. Leyshon, D. Saunders, M. V. Mijovic, A. Bright and J. Bogie (1972) Fluorescence of aromatic benzoxazole derivatives. *J. Am. Chem. Soc.* **94**, 2414–21.

7. Kanegae, Y., K. Peariso and S. S. Martinez (1996) Class of photostable, highly efficient UV dyes: 2-phenylbenzoxazoles. *Appl. Spectrosc.* **50**, 316–19.
8. Dey, J. K. and S. K. Dogra (1990) Absorption and fluorescence characteristics of some 2-alkyl-benzoxazoles 2-aryl-benzoxazoles in different solvents and at various acid concentrations. *Ind. J. Chem. Sect A* **29**, 1153–64.
9. Dey, J. K. and S. K. Dogra (1990) Spectral characteristics of 3 different isomeric 2-(aminophenyl)benzoxazoles - effect of solvents and acid concentrations. *Chem. Phys.* **143**, 97–107.
10. Del Valle, J. C., M. Kasha and J. Catalan (1997) Spectroscopy of amplified spontaneous emission laser spikes in phenyloxazoles. Prototype Classes. *J. Phys. Chem. A* **101**, 3260–72.
11. Guzow, K., K. Mazurkiewicz, M. Szabelski, R. Ganzynkowicz, J. Karolczak and W. Wiczk (2003) Influence of an aromatic substituent in position 2 on photophysical properties of benzoxazol-5-yl-alanine derivatives. *Chem. Phys.* **295**, 119–30.
12. Pladalmau, A. (1995) 2-(2′-hydroxyphenyl)benzothiazoles, 2-(2′-hydroxyphenyl) benzoxazoles, and 2-(2′-hydroxyphenyl)benzimidazoles for plastic scintillation applications. *J. Org. Chem.* **60**, 5468–73.
13. Wang, Y., K. M. Wang, W. H. Liu, G. L. Shen and R. Q. Yu (1997) Optical chemical sensors for pharmaceutical analysis using 1,4-bis(1,3-benzoxazol-2-yl)benzene as sensing material. *Analyst.* **122**, 69–75.
14. Wang, Y., W. H. Liu, K. M. Wang, G. L. Shen and R. Q. Yu (1998) Optical fiber sensor for berberine based on fluorescence quenching of 2-(4-diphenylyl)-6-phenylbenzoxazole. *Fresen. J. Anal. Chem.* **361**, 827–827.
15. Muir, M. M., O. Cox, L. A. Rivera, M. E. Cadiz and E. Medina (1992) Synthesis and characterization of new platinum(ii) complexes containing thiazole and imidazole donors .3. Dichlorobis(styrylbenzazole)platinum(ii) complexes. *Inorg. Chim. Acta.* **191**, 131–9.
16. Lozano, C. M., O. Cox, M. M. Muir, J. D. Morales, J. L. Rodriguez-Caban, P. E. Vivas-Mejia and F. A. Gonzalez (1998) Cytotoxic anionic tribromo platinum(II) complexes containing benzothiazole and benzoxazole donors: synthesis, characterization, and structure-activity correlation. *Inorg. Chim. Acta.* **271**, 137–44.
17. Oren, I., O. Temiz, I. Yalcin, E. Sener and N. Altanlar (1999) Synthesis and antimicrobial activity of some novel 2,5- and/or 6-substituted benzoxazole and benzimidazole derivatives. *Eur. J. Pharm. Sci.* **7**, 153–60.
18. Sener, E. A., O. T. Arpaci, I. Yalcin and N. Altanlar (2000) Synthesis and microbiological activity of some novel 5-benzamido- and 5-phenylacetamido- substituted 2-phenylbenzoxazole derivatives. *Farmaco* **55**, 397–405.
19. Oksuzoglu, E., B. Tekiner-Gulbas, S. Alper, O. Temiz-Arpaci, T. Ertan, I. Yildiz, N. Diril, E. Sener-Aki and I. Yalcin (2008) Some benzoxazoles and benzimidazoles as DNA topoisomerase I and II inhibitors. *J. Enzym. Inhib. Med. Chem.* **23**, 37–42.
20. Oksuzoglu, E., O. Temiz-Arpaci, B. Tekiner-Gulbas, H. Eroglu, G. Sen, S. Alper, I. Yildiz, N. Diril, E. Aki-Sener and I. Yalcin (2007) A study on the genotoxic activities of some new benzoxazoles. *Med. Chem. Res.* **16**, 1–14.
21. Liang, S. C., H. Wang, Z. M. Zhang, X. Zhang and H. S. Zhang (2002) Direct spectrofluorimetric determination of glutathione in biological samples using 5-maleimidyl-2-(m-methylphenyl) benzoxazole. *Anal. Chim. Acta.* **451**, 211–19.
22. Liang, S. C., H. Wang, Z. M. Zhang and H. S. Zhang (2005) Determination of thiol by high-performance liquid chromatography and fluorescence detection with 5-methyl-(2-(m-iodoacetylaminophenyl) benzoxazole. *Anal. Bioanal. Chem.* **381**, 1095–100.
23. Liang, S. C., H. Wang, Z. M. Zhang, M. Zhang and H. S. Zhang (2002) Spectrofluorimetric determination of cysteine by 5-maleimidyl-2-(m-methylphenyl)benzoxazole. *Spectrochim. Acta. A* **58**, 2605–11.
24. Szabelski, M., M. Rogiewicz and W. Wiczk (2005) Fluorogenic peptide substrates containing benzoxazol-5-yl-alanine derivatives for kinetic assay of cysteine proteases. *Anal. Biochem.* **342**, 20–7.
25. Tanaka, K., T. Kumagai, H. Aoki, M. Deguchi and S. Iwata (2001) Application of 2-(3,5,6-trifluoro-2-hydroxy-4-methoxyphenyl)benzoxazole and -benzothiazole to fluorescent probes sensing pH and metal cations. *J. Org. Chem.* **66**, 7328–33.
26. Milewska, M., A. Skwierawska, K. Guzow, D. Smigiel and W. Wiczk (2005) [2-2-quinoxalinyl]benzoxazol-5-yl]alanine derivative - A specific fluoroionophore for Ni(II). *Inorg. Chem. Comm.* **8**, 947–50.
27. Guzow, K., M. Szabelski, J. Malicka, J. Karolczak and W. Wiczk (2002) Synthesis and photophysical properties of 3-[2-[pyridyl]benzoxazol-5-yl]-L-alanine derivatives. *Tetrahedron* **58**, 2201–9.
28. Guzow, K., D. Szmigiel, D. Wroblewski, M. Milewska, J. Karolczak and W. Wiczk (2007) New fluorescent probes based on 3-(2-benzoxazol-5-yl) alanine skeleton - Synthesis and photophysical properties. *J. Photochem. Photobiol. A Chem.* **187**, 87–96.
29. Fayed, T. A. (2004) Probing of micellar and biological systems using 2-(p-dimethylaminostyryl)benzoxazole - An intramolecular charge transfer fluorescent probe. *Colloid Surf. A* **236**, 171–7.
30. Park, K. H., J. T. Lim, S. Song, Y. S. Lee, C. J. Lee and N. Kim (1999) Nonlinear optical polymers with novel benzoxazole chromophores IV. Synthesis of maleimide-styrene and maleimide-methacrylate copolymers. *React. Funct. Polym.* **40**, 177–84.
31. Centore, R., S. Concilio, B. Panunzi, A. Sirigu and N. Tirelli (1999) Nonlinear optical properties of some side chain copolymers based on benzoxazole containing chromophores. *J. Polym. Sci. Pol. Chem.* **37**, 603–8.
32. Hsu, S. L. C. and W. C. Chen (2002) A novel positive photosensitive polybenzoxazole precursor for microelectronic applications. *Polymer* **43**, 6743–50.
33. Hong, H. W. and T. M. Chen (2007) Effect of substituents on the photoluminescent and electroluminescent properties of substituted cyclometalated iridium(III) complexes. *Mater. Chem. Phys.* **101**, 170–6.
34. Gimenez, R., L. Oriol, M. Pinol, J. L. Serrano, A. I. Vinuales, T. Fisher and J. Stumpe (2006) Synthesis and properties of 2-phenylbenzoxazole-based luminophores for in situ photopolymerized liquid-crystal films. *Helv. Chim. Acta.* **89**, 304–19.
35. Lown, J. W. and J. P. Moser (1970) The 1,3-dipolar addition of 2-aroyl-aziridines to 1-nitrosonaphth-2-ol: novel syntheses of substituted naphtho[1,2-d]oxazoles. *J. Chem. Soc. Chem. Commun.* **24**, 7–248.
36. Lown, J. W. and J. P. Moser (1970) 1,3-dipolar cycloaddition of nitrosonaphthols to 3-aroylazindines. Novel syntheses of substituted naphtho[1,2-d]oxazoles and naphtho[2,1-d]oxazoles. *Can. J. Chem.* **48**, 2227–33.
37. Perry, R. J., B. D. Wilson and R. J. Miller (1992) Synthesis of 2-arylbenzoxazoles via the palladium-catalyzed carbonylation and condensation of aromatic halides and ortho-aminophenols. *J. Org. Chem.* **57**, 2883–7.
38. Saitz, C., H. Rodriguez, A. Marquez, A. Canete, C. Jullian and A. Zanocco (2001) New synthesis of naphtho- and benzoxazoles: decomposition of naphtho- and benzoxazinones with KOH. *Synth. Commun.* **31**, 135–40.
39. Chang, J. B., K. Zhao and S. F. Pan (2002) Synthesis of 2-arylbenzoxazoles via DDQ promoted oxidative cyclization of phenolic Schiff bases - a solution-phase strategy for library synthesis. *Tetrahedron. Lett.* **43**, 951–4.
40. Li, H., K. Wei and Y. J. Wu (2007) A convenient synthesis of 2-arylnaphtho(1,2-d]oxazole derivatives promoted by triethylamine. *Chin. J. Chem.* **25**, 1704–9.
41. Benniston, A. C., A. Harriman and K. S. Gulliya (1994) Photophysical properties of merocyanine 540 derivatives. *J. Chem. Soc. Faraday. Trans.* **90**, 953–61.
42. You, Y., J. Seo, S. H. Kim, K. S. Kim, T. K. Ahn, D. Kim and S. Y. Park (2008) Highly phosphorescent iridium complexes with chromophoric 2-(2-hydroxyphenyl)oxazole-based ancillary ligands: Interligand energy-harvesting phosphorescence. *Inorg. Chem.* **47**, 1476–87.
43. Eaton, D. F. (1988) Reference materials for fluorescence measurement. *Pure Appl. Chem.* **60**, 1107–14.
44. Demas, J. N. and G. A. Crosby (1971) Measurement of photoluminescence quantum yields. *Rev. J. Phys. Chem.* **75**, 991–1024.
45. Frisch M. J., H. B. Schlegel, G. E. Scuseria, M. A. Robb, J. R. Cheeseman, J. A. Montgomery Jr., T. Vreven, K. N. Kudin, J. C. Burant, J. M. Millam, S. S. Iyengar, J. Tomasi, V. Barone, B. Mennucci, M. Cossi, G. Scalmani, N. Rega, G. A. Petersson, H. Nakatsuji, M. Hada, M. Ehara, K. Toyota, R. Fukuda, J. Hasegawa, M. Ishida, T. Nakajima, Y. Honda, O. Kitao, H. Nakai, M. Klene, X. Li, J. E. Knox, H. P. Hratchian, J. B. Cross, C. Adamo, J. Jaramillo,

R. Gomperts, R. E. Stratmann, O. Yazyev, A. J. Austin, R. Cammi, C. Pomelli, J. W. Ochterski, P. Y. Ayala, K. Morokuma, G. A. Voth, P. Salvador, J. J. Dannenberg, V. G. Zakrzewski, S. Dapprich, A. D. Daniels, M. C. Strain, O. Farkas, D. K. Malick, A. D. Rabuck, K. Raghavachari, J. B. Foresman, J. V. Ortiz, Q. Cui, A. G. Baboul, S. Clifford, J. Cioslowski, B. B. Stefanov, G. Liu, A. Liashenko, P. Piskorz, I. Komaromi, R. L. Martin, D. J. Fox, T. Keith, M. A. Al-Laham, C. Y. Peng, A. Nanayakkara, M. Challacombe, P. M. W. Gill, B. Johnson, W. Chen, M. W. Wong, C. Gonzalez and J. A. Pople (2003) Gaussian 03W, Rev. B. 03., Gaussian, Inc., Pittsburgh PA.

46. da Hora Machado, A. E., J. A. de Miranda, S. Guilardi, D. E. Nicodem and D. Severino (2003) Photophysics and spectroscopic properties of 3-benzoxazol-2-yl-chromen-2-one. *Spectrochim. Acta A* **59**, 345–55.
47. Le Bris, M. (1985) Synthesis and properties of some 7-dimethylamino-1,4-benzoxazin-2-ones. *J. Heterocyclic Chem.* **22**, 1275–81.
48. Kovac, B. and I. Novak (2002) Electronic structure of coumarins. *Spectroc. Acta. A* **58**, 1483–8.
49. Reichardt, C. (1990) *Solvents and Solvent Effects in Organic Chemistry*. 2th Edition, VCH, Weinheim.
50. Kamlet, M. J., J.-L. M. Abboud, M. H. Abraham and R. W. Taft (1983) Linear solvation energy relationships. 23. A comprehensive collection of the solvatochromic parameters, .pi.*, .alpha., and .beta., and some methods for simplifying the generalized solvatochromic equation. *J. Org. Chem.* **48**, 2877–87.
51. Barton, A. F. M. (1975) Solubility parameters. *Chem. Rev.* **75**, 731–53.
52. Abraham, M. H., R. M. Doherty, M. J. Kamlet, J. M. Harris and R. W. Taft (1987) Linear solvation energy relationships Part 37. An analysis of contributions of dipolarity–polarisability, nucleophilic assistance, electrophilic assistance, and cavity terms to solvent effects on t-butyl halide solvolysis rates. *J. Chem. Soc. Perkin. Trans.* **2**, 913–20.
53. Kamlet, M. J., P. W. Carr, R. W. Taft and M. H. Abraham (1981) Linear solvation energy relationships. 13 Relationship between the Hildebrand solubility parameter, .delta.H, and the solvatochromic parameter, .pi.*. *J. Am. Chem. Soc.* **103**, 6060–6.
54. Belsley, D. A., E. Kuh and R. E. Welsch (1980) *Regression Diagnostics: Identifying Influential Data and Sources of Collinearity*. John Wiley & Sons, New York.
55. Cronce, D. T., G. R. Famini, J. A. De Soto and L. Y. J. Wilson (1998) Using theoretical descriptors in quantitative structure-property relationships: some distribution equilibria. *J. Chem. Soc. Perkin. Trans.* **2**, 1293–301.
56. Famini, G. R. and C. A. Penski (1992) Using theoretical descriptors in quantitative structure-activity-relationships - some physicochemical properties. *J. Phys. Org. Chem.* **5**, 395–408.
57. Famini, G. R. and L. Y. Wilson (1994) Using theoretical descriptors in quantitative structure-property relationships - 3-carboxybenzisoxazole decarboxylation kinetics. *J. Chem. Soc. Perkin. Trans.* **2**, 1641–50.
58. Krishnamoorthy, G. and S. K. Dograr (1999) Dual fluorescence of 2-(4′-N,N-dimethylaminophenyl)benzoxazole: Effect of solvent and pH. *Chem. Phys.* **243**, 45–59.
59. Rettig, W., M. Vogel, E. Lippert and H. Otto (1986) The dynamics of adiabatic photoreactions as studied by means of the time structure of synchrotron radiation. *Chem. Phys.* **103**, 381–90.
60. Changenet, P., P. Plaza, M. M. Martin and Y. H. Meyer (1997) Role of intramolecular torsion and solvent dynamics in the charge-transfer kinetics in triphenylphosphine oxide derivatives and DMABN. *J. Phys. Chem.* **101**, 8186–94.
61. Lippert, E. (1957) Spektroskopische Bestimmung des Dipolmomentes aromatischer Verbindungen im ersten angeregten Singulettzustand. *Z. Electrochem.* **61**, 962–75.
62. Mataga, N., Y. Kaifu and M. Koizumi (1956) Solvent effects upon fluorescence spectra and the dipole moments of excited molecules. *Bull. Chem. Soc. Jpn.* **29**, 465–70.
63. Etaiw, S. E. D., T. A. Fayed and N. Z. Saleh (2006) Photophysics of benzazole derived push-pull butadienes: A highly sensitive fluorescence probes. *J. Photochem. Photobiol. A* **177**(23), 8–247.
64. Mac, M., B. Tokarczyk, T. Uchac and A. Danel (2007) Charge transfer fluorescence of benzoxazol derivatives Investigation of solvent effect on fluorescence of these dyes. *J. Photochem. Photobiol. A* **191**(3), 2–41.
65. Chaudhuri, R., J. Guharay and P. K. Sengupta (1996) Fluorescence polarization anisotropy as a novel tool for the determination of critical micellar concentrations. *J. Photochem. Photobiol. A* **101**, 241–4.
66. Sharkar, N., A. Datta, S. Das and K. Bhattacharyya (1996) Solvation dynamics of coumarin 480 in micelles. *J. Phys. Chem.* **100**, 15483–6.
67. Heerklotz, H. and J. Seelig (2000) Correlation of membrane/water partition coefficients of detergents with the critical micelle concentration. *Biophys. J.* **78**, 2435–40.
68. Becerra, N., C. Toro, A. L. Zanocco, E. Lemp and G. Gunther (2008) Characterization of micelles formed by sucrose 6-O-monoesters. *Colloids Surf. A* **327**, 134–9.